Korean J. Chem. Eng., **16**(3), 292-297 (1999)

Effect of Initial Droplet Size Distribution on Sulfur Removal Efficiency in FGD/SDA

Eui-Kyung Oh, Gi-Hune Jung, Sun-Geon Kim†, Hyung-Keun Lee* and In-Won Kim**

Department of Chemical Engineering, Chung Ang University, 221, Huksuk-Dong, Dongjak-Ku, Seoul 156-756, Korea
*Energy and Environmental Research Department, Korea Institute of Energy Research,
71-2, Jang-Dong, Yusong-Ku, Taejon 305-343, Korea
**Department of Chemical Engineering, Kon Kuk University, 93-1, Mojin-Dong, Kwangjin-Ku, Seoul 143-701, Korea
(*Received 5 August 1998 • accepted 22 February 1999*)

Abstract–Dry scrubbing with lime slurry in a spray dryer [spray dryer absorber (SDA)] has been an important technology for flue gas desulfurization (FGD). Mathematical models based on the heat and mass balances are used to predict SO_2 removal in the SDA as a function of initial size distribution of slurry droplets. Since the existence of moisture in the droplets appreciably enhances the SO_2 removal, its removal efficiency depends on the rate of drying as well as that of SO_2 removal itself, both depending on droplet diameter. With the increase in the geometric standard deviation (GSD) of the initial droplet size distribution, the efficiency of SO_2 removal first increases and then decreases, showing a maximum at a certain value of GSD. This trend is altered by the sorbent content of the droplets, expressed as stoichiometric ratio (SR). The decrease in SR makes the maximum move to higher GSD and reduces the variation in the efficiency with respect to GSD. For SR<0.73, a minimum efficiency also appears, ahead of the maximum. The results are well explained by the specific rates of both drying and SO_2 removal of the droplets.

Key words : Flue Gas Desulfurization, Spray Dryer Absorber, Modeling, Droplet Size Distribution, Drying, SO_2 Removal

INTRODUCTION

In semi-dry FGD processes, the slurry droplets containing sorbent particles are sprayed to reactively absorb SO_2 in flue gas while drying by sensible heat of the gas. Dry and spent sorbent particles are either disposed of or recovered. Without a doubt, the initial size distribution of the droplets plays a very important role in the series of processes described above and consequently in SO_2 removal [Klingspor et al., 1983].

Although many types of spray have been developed, producing quite different size distribution of droplets, there have been very few studies on their size effect. Jozewicz and Rochelle [1984] calculated the time needed to evaporate 99 % of the polydisperse spray. They showed the time does not differ significantly from that needed for evaporating monodisperse sprays for low values of standard deviation, but the time rises dramatically for a standard deviation (expressed in ln s_g) larger than 1.0 (or $s_g > 2.72$). They also calculated SO_2 removal as a function of the approach temperature to saturation for different lime stoichiometry, which is defined as the ratio of the total moles of $Ca(OH)_2$ to the moles of SO_2 in the flue gas. All the results were obtained for the spray of a standard deviation (ln s_g) of 1.56 (which can be converted to $s_g = 4.76$, an uncommonly large value) assuming an infinite rate of $Ca(OH)_2$ dissolution. At stoichiometry >1.5 the removal of SO_2 was the same as predicted by a simple concurrent model without size distribution. At low stoichiometry and close approach to the saturation temperature, all of the $Ca(OH)_2$ was utilized. Their results are, however, too qualitative and unrealistic to generalize and apply practically.

In order to get a clear idea of the droplet size effect on the SDA performance, we quantitatively investigated the effect of polydispersity on the evaporation of water, removal efficiency of SO_2, and thus sorbent utilization in SDA, modifying the previous model [Jang et al., 1996].

FUNDAMENTAL EQUATIONS AND NUMERICAL APPROACH

In our model, the slurry droplets containing $Ca(OH)_2$ as sorbent particles are sprayed in the top of the SDA and the flue gas consisting of nitrogen, water vapor and SO_2 is introduced above the spray. Since the sprayed droplets injected radially lose their velocities in an extremely short period of time, the flow of both the gas and droplets is assumed concurrent and plug flow. We also assume there is neither circulation nor temperature distribution in a droplet and neglect heat loss across the SDA wall. The size distribution function of the sprayed droplets, $f(d_d)$ is assumed lognormal, whose applicability has been proven :

$$f(d_d) = \frac{1}{\sqrt{2p}\,\ln s_g}\exp\left[-\frac{(\ln d_d - \ln d_g)^2}{2(\ln s_g)^2}\right] \quad (1)$$

where s_g is the geometric standard deviation, d_d the droplet diameter and d_g the geometric mean diameter of droplets. All the assumptions above are the same as those of Partridge, 1987; Shih, 1989; Kolluri, 1991 and Yuan, 1990.

1. Rate of SO_2 Removal

The rate of SO_2 removal by droplets can be expressed as

†To whom correspondence should be addressed.
E-mail : sgkim@cau.ac.kr

[Kolluri, 1991] :

$$m_s = \frac{p d_d^2 \left[C_{l,c} \left(\frac{D_{l,c}}{D_{l,s}} \right) + \frac{C_{g,s}}{H} \right]}{\frac{1}{k_{l,s}} + \frac{1}{H k_{g,s}} + \frac{p d_d^2 d R_L}{D_{l,c} N_p p d_p^2}} \quad (2)$$

where $C_{l,c}$ and $C_{g,s}$ are the concentrations of sorbent and SO_2 in liquid and gas phases, respectively, $D_{l,s}$ and $D_{l,c}$ are the diffusion coefficients of SO_2 and sorbent in the liquid phase, respectively ; H is the Henry's law constant ; $k_{l,s}$ and $k_{g,s}$ are the mass transfer coefficients of SO_2 in liquid and gas phases, respectively ; d the hypothetical thickness of the liquid film sur-rounding the sorbent particle ; R_L is the fraction of the sorbent unreacted in the sorbent particle and N_p is the number of sorbent particles in a droplet. Eq. (2) can be used only if the moisture content (X) of the droplet exceeds a certain value, X_u, while for $X < X_u$, the rate of SO_2 removal is calculated by gas-solid reaction, $m_s = k_s C_{g,s}$ where k_g is the constant of the gas-solid reaction. The threshold moisture content, X_u is estimated by $X_u = 6.1 * RH * X_e$ [Shih, 1989], where RH is the relative humidity of outlet flue gas and X_e is the equilibrium moisture content of the sorbent particle.

2. Governing Equations

The structure of the governing equations is almost unchanged compared with those appearing in our previous publication [Jang et al., 1996]. The droplet-phase variables in the gas-phase balance equations are, however, expressed in the forms integrated with respect to the diameter of the droplets.

The balance for the mass of the sorbent $Ca(OH)_2$ (m_c) in a droplet with a diameter of d_d is :

$$\frac{dm_c(d_d)}{dt} = -\frac{\cdot m_s(d_d)}{i_c} \quad (3)$$

where i_c is the stoichiometric ratio of SO_2 to $Ca(OH)_2$ based on mass.

The balance for the mass of water (m_w) in a droplet with a diameter of d_d is :

$$\frac{dm_w(d_d)}{dt} = -\frac{\cdot m_s(d_d)}{i_w} - m_w(d_d) \quad (4)$$

where i_w is the stoichiometric ratio of SO_2 to water based on mass, and m_w is the drying rate of water. The rate is expressed according to the types of drying-rate period, respectively, as [Partridge, 1987] :

$$m_s(d_d) = 2p C_t d_d D_{g,w} \ln \frac{1 - y_{g,w}}{1 - y_{i,w}} \quad \text{for constant drying-rate period} \quad (5)$$

$$m_s(d_d) = 2p C_t d_d D_{g,w} \ln \frac{1 - y_{g,w}}{1 - y_{i,w}} \frac{X - X_e}{X_c - X_e}$$

$$\text{for falling drying-rate period} \quad (6)$$

where C_t is the total molar concentration of the gas phase, $y_{g,w}$ and $y_{i,w}$ are the mole fractions of water vapor in bulk gas and at the surface of the droplet, respectively, and $D_{g,w}$ is the diffusion coefficient of water vapor in the gas phase. The transition from the constant drying-rate period to the falling drying-rate period occurs at the critical moisture content, X_c.

The energy balance for a slurry droplet with a diameter of d_d consisting of sensible heat supply from the gas phase, latent and sensible heat consumption by water evaporation, and heat effect from dissolution of gaseous SO_2 into the droplet, is :

$$\frac{d[m_d(d_d) c_{p,d}(d_d) T_d(d_d)]}{dt} = -m_w(d_d) h_w + m_s(d_d) h_s + p d_d^2 h_t(d_d)[T_\infty - T_d(d_d)] \quad (7)$$

where m_d, $c_{p,d}$ and T_d are the mass, specific heat and temperature of the droplet with a diameter of d_d, respectively, h_w and h_s are the specific enthalpies of water vapor and gas-phase SO_2, respectively, h_t the heat transfer coefficient in the gas phase, and T_∞ the gas temperature.

The SO_2 mass balance in the gas phase is :

$$\frac{dm_{g,s}}{dt} = N \int_0^\infty i_c \frac{dm_c(d_d)}{dt} f(d_d) dd_d \quad (8)$$

where $m_{g,s}$ is the mass flow rate of SO_2 in the flue gas, N the total number flow rate of droplets (number of droplets/sec) and the integral term represents the mean rate of SO_2 removal over the whole spectrum of droplet size.

On the other hand, the humidity (Y_∞) balance in the flue gas gives :

$$m_g \frac{dH_\infty}{dt} = N \int_0^\infty m_w(d_d) f(d_d) dd_d \quad (9)$$

where m_g is the mass flow rate of dry flue gas. The integral term again represents the mean rate of drying over the whole spectrum of droplet size.

The energy balance equation in the gas phase, consisting of sensible heat supply out of the flue gas, and latent and sensible heat effects arising from water evaporation, is :

$$\frac{d(m_\infty c_{p,\infty} T_\infty)}{dt} = N \int_0^\infty [m_w(d_d) H_w - p d_d^2 h_t(d_d)[T_\infty - T_d(d_d)] - m_s(d_d) H_s] f(d_d) dd_d \quad (10)$$

where m_∞ and $c_{p,\infty}$ are the flow rate and constant-pressure specific heat of total gas, respectively. The right-hand side term also contains an integral form over the whole size spectrum.

3. Numerical Scheme

The whole spectrum of droplet size approximately in the range of $\ln d_g \pm 3 \ln s_g$ is divided equally in logarithmic scale into 11 classes. For Eqs. (3), (4) and (7), each class of size has corresponding expressions to yield a total of 3×11 ordinary differential equations. For Eqs. (8), (9) and (10) for the flue gas, the integral terms in the right-hand side are calculated numerically. All the equations are rewritten in terms of vertical distance instead of time by the following relationship :

$$dt = \frac{dz}{U_d(d_d)} \quad (11)$$

where U_d is the droplet velocity. As proved in our previous study [Jang et al., 1996], the droplet velocity is assumed equal to the gas velocity U_∞, which is recalculated at each iteration.

Table 1. Baseline condition

Parameters	Base-line value
Inlet gas temperature	145 °C
% water vapor in inlet gas	5 %
In let SO_2 concentration in the gas	913 ppm
Approach temperature to saturation	11 °C
Stoichiometric ratio	1
Residence time	15.2 sec
Inlet droplet diameter	82 *m*m
Inlet droplet temperature	37.8 °C
Inlet sorbent particle diameter	1.25 *m*m
Critical moisture content	29.2 %
Equilibrium moisture content	6 %

The axial distance is then normalized by the total SDA length.

The thirty-six ordinary differential equations are then solved by LSODE package, one of the initial-value ODE solvers. The sorbent particles in our study are monodisperse and their size is fixed, as shown in Table 1. Their number in each droplet is proportional to its volume (d_d^3) for the given SR.

The SDA data used in this study are Partridge's baseline conditions, which have been quoted by many authors [Partridge, 1987; Shih, 1989; Yuan, 1990]. Partridge's apparatus has a diameter of 2.13 m, a length of 2.5 m. Table 1 shows the baseline condition set up by Partridge.

The initial droplet diameter shown in Table 1 is used as the geometric mean diameter d_g. The geometric standard deviations range from 1.00001 (close to monodispersity) to 2.0. The variables in Table 1 are all set to their baseline values except the stoichiometric ratio (SR) which is the most significant variable for the SO_2 removal [Jang et al., 1996]. SR varies from 0.6 to 2.0.

RESULTS AND DISCUSSION

Fig. 1 shows the initial size distributions of droplets for three different values of GSD (s_g). The geometric mean diameter of the droplets fixed at 82×10^{-6} m is the same as the diameter of monodisperse droplets (s_g=1.0). For s_g=1.2, the droplet size

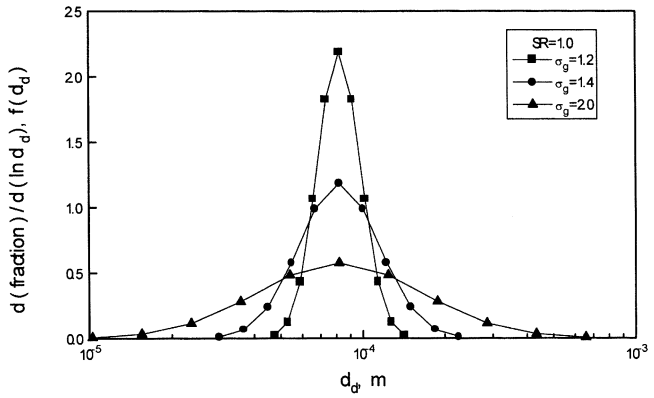

Fig. 1. Variation in droplet size distribution with respect to dimensionless axial length, Z (SR=1.0, s_g=1.35).

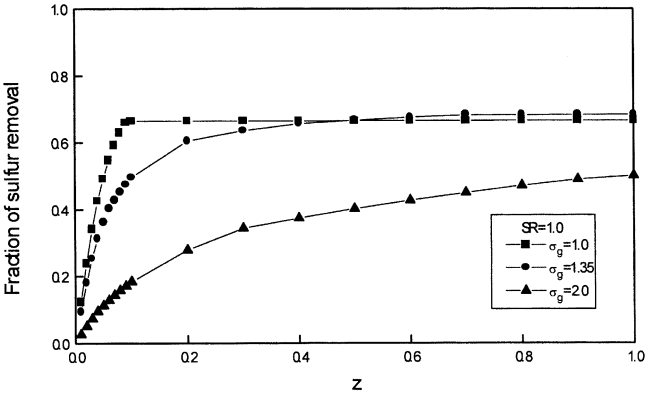

Fig. 2. Variation in droplet size distribution with respect to dimensionless axial length, Z (SR=1.0, s_g=2.0).

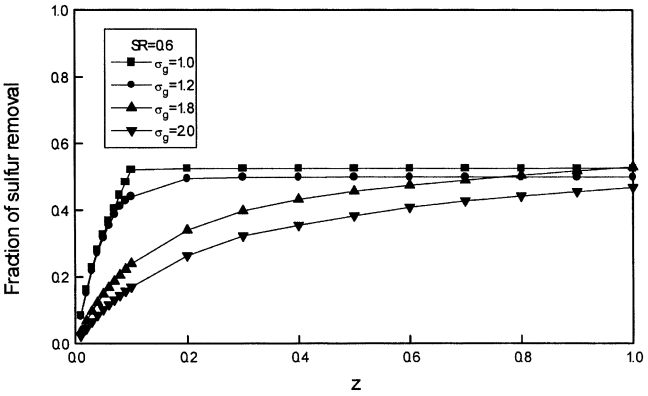

Fig. 3. Effect of initial geometric standard deviation of droplet size distribution, s_g on exit flue-gas humidity.

ranges from 50×10^{-6} m to 140×10^{-6}m, for s_g=1.4, from 30×10^{-6} m to 250×10^{-6} m, and for s_g=2.0, from 10×10^{-6} m to 650×10^{-6} m. Figs. 2 and 3 show the axial distributions of the fraction of sulfur removal in the flue gas, as a parameter of GSD, for SR= 1.0 and SR=0.6, respectively. For monodisperse droplets, the variations in both cease very close to the inlet, but the increase in GSD spreads out their variations further towards the SDA outlet. The figures also show that the fraction for SR=1.0 and s_g= 1.35 exceeds that for monodisperse droplets around the middle of the SDA while the fraction for SR=0.6 and s_g=1.80 does near the outlet of the SDA. The reasons why will be explained later.

1. The Effect of Size Distribution of Slurry Droplets on Their Drying

Fig. 4 shows the variation in droplet size distribution along the SDA axis for the initial s_g=1.35. Since, as shown in Eqs. (5) and (6), the rate of drying per unit droplet is proportional to d_d, the corresponding specific rate (rate per mass of droplet) is inversely proportional to d_d^2. Therefore, the smaller the droplets, the earlier they dry up. As a result, along the axis, the size distribution of the droplets becomes, in turn, skewed with long head (Z=0.01), symmetrical (lognormal) but broader than the initial one (Z=0.05), and skewed with long tail (Z=0.1, 0.5). Finally the lognormal distribution with the initial broadness is recovered (Z=1.0), as all the droplets dry up. In Fig. 5 for the

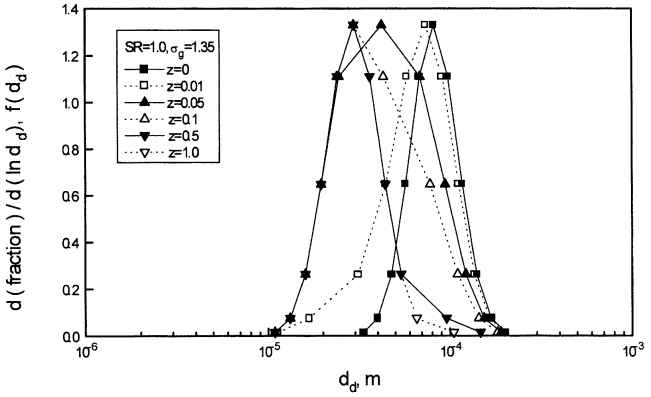

Fig. 4. Effect of initial geometric standard deviation of droplet size distribution, s_g on exit flue-gas temperature.

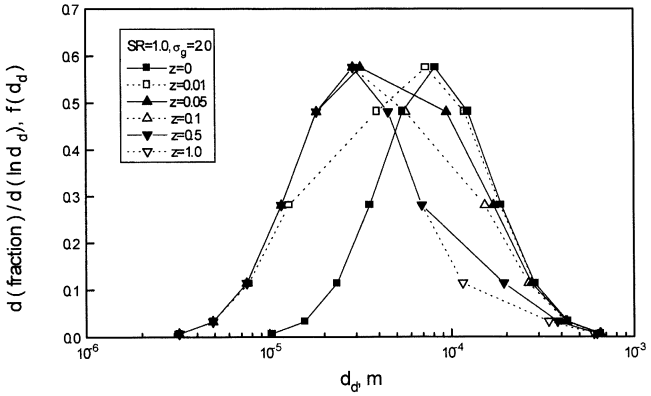

Fig. 5. Effect of initial geometric standard deviation of droplet size distribution on sulfur removal efficiency as a parameter of SR.

distribution of s_g=2.0, similar trends are observed. However, the large droplets in the broadened distribution do not dry completely even at the outlet and the distribution ends up with a long tail.

Fig. 6 shows the effect of droplet size distribution on the flue gas humidity at the SDA outlet, as a parameter of SR. The distribution effect is hardly observed for the systems with s_g<1.4, where most droplets dry up within SDA. However, for s_g>1.4, the humidity decreases appreciably with s_g due to

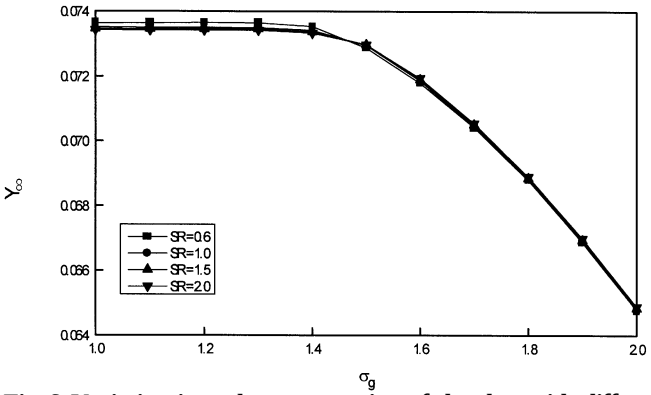

Fig. 6. Variation in sorbent conversion of droplets with different sizes along SDA axis (SR=1.0, s_g=1.35).

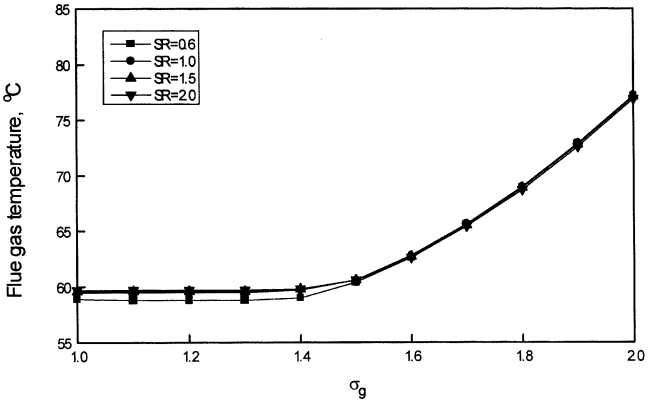

Fig. 7. Variation in sorbent conversion of droplets with different sizes along SDA axis (SR=1.0, s_g=2.0).

the incomplete drying, as described above. For the systems with narrower distribution (s_g<1.4), the increase in the sorbent mass (SR) slightly decreases the humidity since the sorbent needs more equilibrium moisture which cannot eventually evaporate from the droplets. It is suggested that the effect is obscured for the systems with broader distribution, due to the incomplete drying. The effect of size distribution on the flue gas temperature, shown in Fig. 7, is reversed, since the gas humidity increases at the expense of the sensible heat of the gas.

2. The Effect of Size Distribution on SO_2 Removal Efficiency

Fig. 8 shows the conversion of sorbent particles in each class of droplets along the SDA axis for the system with SR=1 and the initial s_g=1.35. As shown in Eq. (2), the rate of SO_2 removal per unit droplet is proportional to d_d^2, when the third term in the denominator in right-hand side (sorbent dissolution term) is neglected. If the term is dominant, the SO_2 removal is proportional to d_d^3, since N_p is proportional to d_d^3. The corresponding specific rates (rates per mass of droplet) are, therefore, inversely proportional to d_d^n ($n \leq 1$). Due to higher size-dependence of drying (inversely proportional to d_d^2) than SO_2 removal, the drying of smaller droplets occurs much faster than their SO_2 removal (thus, their sorbent conversion) does. As described in a previous paper [Jang et al., 1996], the SO_2 removal is appreciable only for the droplets having free mois-

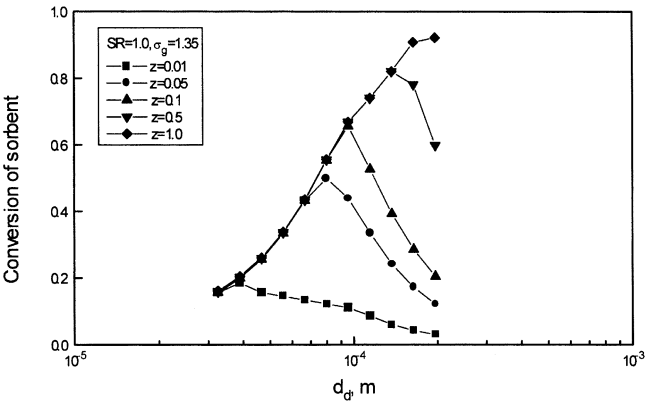

Fig. 8. Variation in sorbent conversion of droplets with different sizes along SDA axis (SR=1.0, s_g=1.35).

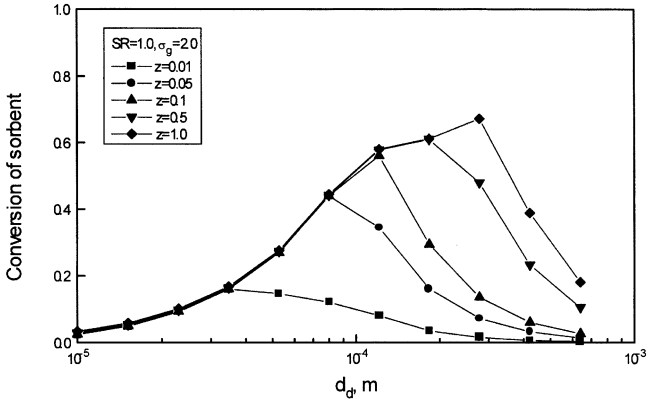

Fig. 9. Variation in sorbent conversion of droplets with different sizes along SDA axis (SR=1.0, s_g=2.0).

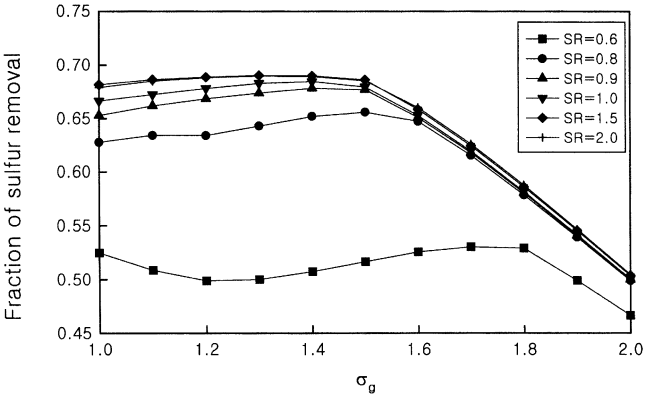

Fig. 10. Effect of initial geometric standard deviation of droplet size distribution on sulfur removal efficiency as a parameter of SR.

ture. Therefore, the smaller droplets have higher conversion as far as the moisture is retained in them, but their conversion is almost frozen as soon as their drying ends up. On the other hand, larger droplets retain moisture much longer than smaller ones and have more opportunity to enhance their conversion by the reaction with SO_2. As shown in the figure, the droplet size showing maximum conversion, therefore, moves to the larger one along the SDA axis and, at the outlet, the largest droplet has the highest conversion, since it has almost dried up (Fig. 4). Fig. 9 shows the results for s_g=2.0. Compared to Fig. 8, the conversions for the droplets in the lower part of the broadened distribution are frozen at lower values due to their increased drying rates. On the other hand, since the droplets in the upper part of the distribution are not completely dried (Fig. 5), their conversions decrease with the diameter of the droplets, as described above. Therefore, the largest droplets do not have the highest conversion even at the exit of the SDA.

The broadening effect of the droplet size distribution on the overall SO_2 removal efficiency, therefore, appears somewhat complicated. It depends on whether the loss of SO_2 removal capacity in the smaller droplets can be recovered by its gain in the larger droplets or not. Fig. 10 shows the effect of size distribution on SO_2 removal efficiency as a parameter of SR. For SR>0.73, the efficiency increases with GSD (s_g) up to a maximum and then greatly decreases to a much lower value than the monodisperse (s_g=1) efficiency. For SR>1.0, the SO_2 removal efficiency ranges from 50 to 70 %. It is suggested that the slight broadening of the size distribution increases the time of water retention in larger droplets, which leads to a greater chance for SO_2 removal as a whole, and makes the gain in larger-sized droplets exceed the loss in lower-sized ones more and more. However, with further increase in s_g, the overall removal efficiency declines since the gain is substantially reduced and cannot recover the loss due to the reduction in the rate of SO_2 removal, as described before (inversely proportional to d_d^n, where n<1).

With the reduction of sorbent content (SR), the GSD showing the maximum efficiency ($s_{g,\,max}$) moves to a higher value. It is suggested that the decrease in SR reduces the rate of SO_2 removal, due to the decrease in both the number (N_p) and liquid-phase concentrations ($C_{l,c}$) of sorbent particles [Eq. (2)], and makes the removal rate more controlled by sorbent dissolution. Therefore, SO_2 removal depends less on the droplet diameter, since n decreases from unity in the size dependence of its specific rate, d_d^{-n}. As a result, for lower SR the decline of the efficiency begins at higher GSD. Further reduction in SR below 0.73 shows a minimum efficiency at a certain value of $s_g < s_{g,\,max}$. This implies that such a small increase in broadness is not sufficient for the positive effect on the SO_2 removal in the upper part of the distribution to exceed the negative effect in the lower part, due to much lowered rate of SO_2 removal. This and the lowered dependence on the diameter make the efficiency variation with respect to GSD appreciably reduced. For example, for SR=0.6, the SO_2 removal efficiency decreases up to s_g=1.2, then increases to a maximum at s_g=1.8 and finally decreases afterwards, and the efficiency varies only between 46 and 53 %.

CONCLUSION

We have numerically investigated the effect of the droplet size distribution on the SO_2 removal efficiency of the spray dryer absorber (SDA). In general, the size distribution affects the efficiency through the variation in both the moisture-retention ability and SO_2 removal rate of the droplets.

1. The size distribution of droplets becomes distorted and broader until their drying is completed.
2. High polydispersity makes the exit gas humidity fall and the exit gas temperature rise.
3. The droplets, which are about to dry up, have the highest conversion. The size of the droplets with maximum conversion becomes larger along the SDA axis.
4. The effect of size distribution on SO_2 removal efficiency becomes significant with the stoichiometric ratio of sorbent to SO_2. For SR>0.73, the slight broadening in the distribution enhances the SO_2 removal efficiency, while a further increase in s_g significantly lowers the efficiency. The maximum efficiency moves to higher σ_g with the reduction in SR.
5. For SR<0.73, the droplet size distribution affects the re-

moval efficiency less, though showing both the minimum and maximum efficiencies with respect to the standard geometric deviation of droplet size distribution.

ACKNOWLEDGEMENT

This work was supported by Electrical Engineering and Science Research Institute in Seoul National University (96-050).

REFERENCES

Jang, S. H., Oh, E. K., Lee, H. K. and Kim, S. G., "Model Development of Spray Dryer Absorber FGD Process," *Clean Technology* (Korean), **2**, 80 (1996).

Jozewicz, W. and Rochelle, G. T., "Modeling of SO_2 Removed by Spray Dryers," Proc. First Annual Pittsburgh Coal Conf., Sept. 17-21, 663 (1984).

Klingspor, J., Karlsson, H. T. and Bjerle, I., "A Kinetic Study of the Dry SO_2-Limestone Reaction at Low Temperature," *Chem. Eng. Commun*., **22**, 81 (1983).

Kolluri, R., Hatcher, Jr., W. J. and Jefcoat, L. A., "Simulation of Spray Drying with Reaction : Absorption of Hydrogen Sulfide in Ammoniacal Solution of Zinc Chloride," *Drying Technology*, **9**, 367 (1991).

Partridge, G. P., Jr., "A Mechanistic Spray Dryer Mathematical Model Based on Film Theory to Predict Sulfur-Dioxide Ab-sorption and Reaction by a Calcium Hydroxide Slurry in the Constant Rate Period," Ph.D. Dissertation, Tennessee Univ., Knoxville, U.S.A. (1987).

Shih, H. S., "Simulation of Sulfur-Dioxide Removal via Hydrated Lime Slurries in a Spray Dryer Absorber Flue-Gas Desulfurization System," Ph.D. Dissertation, Alabama Univ., Tuscaloosa, U.S.A. (1989).

Yuan, C. S., "Simultaneous Collection of SO_2 and NO_x via Spray Drying : Using Sodium Based and Calcium Based Sorbents with Select Additives," Ph.D. Dissertation, Univ. of Illinois at Urbana-Champaign, U.S.A. (1990).